# Chaotic State in an Electrodynamic Loudspeaker

**Article** *in* Acta Acustica united with Acustica · July 2008

DOI: 10.3813/AAA.918072

CITATIONS
4

READS
118

**3 authors:**

Ivan Djurek
University of Zagreb
**28** PUBLICATIONS **43** CITATIONS
SEE PROFILE

Antonio Petosić
University of Zagreb
**54** PUBLICATIONS **76** CITATIONS
SEE PROFILE

Danijel Djurek
**61** PUBLICATIONS **307** CITATIONS
SEE PROFILE

**ACTA ACUSTICA UNITED WITH ACUSTICA**
**Vol. 94 (2008) 629 – 635**

DOI 10.3813/AAA.918072

# Chaotic State in an Electrodynamic Loudspeaker

Ivan Djurek[1)], Danijel Djurek[2)], Antonio Petosic[1)]

[1)] Faculty of Electrical Engineering and Computing, Dept. of Electroacoustics, Unska 3, Zagreb, Croatia. ivan.djurek@fer.hr; antonio.petosic@fer.hr.

[2)] AVAC – Alessandro Volta Applied Ceramics, Laboratory for Nonlinear Dynamics, Kesten brijeg 5, Remete, Zagreb, Croatia. danijel.djurek@zg.t-com.hr

*Dedicated on the occasion of Professor Boran Leontic's 80th birthday.*

**Summary**

An electrodynamic loudspeaker has been operated in a nonlinear regime with driving currents $I_0 = 2$–$4$ A. At $I_0 = 4$ A an amplitude cut-off was observed at frequency $f = 46$ Hz. In the next step driving frequencies have been selected in the interval 45–55 Hz, and driving current was then swept until vibration amplitude produced sequences of subharmonics which terminated in the chaotic state. An attempt to explain the chaotic phenomena in terms of forced anharmonic oscillator with elastic stiffness derived from static stress-strain measurement and entering Duffing equation failed. Viscoelastic model proposed by Bennewitz and Rötger was applied, when membrane viscoelasticity and corresponding intrinsic friction term enhance the restoring force of the vibrating system. Such a model supplemented with system parameters and transferred to simulation procedure resulted in a period doubling and bifurcation diagram, which might be brought within the loudspeaker technical performances and qualitative agreements such as would be indicated by observations and measurements.

**PACS no. 43.25.Rq, 43.25.Dc, 43.38.Dv**

## 1. Introduction

An electrodynamic loudspeaker, widely used device in sound reproduction, consists of a membrane suspended attached to a fixed rim and put in motion by the Lorentz force exerted on the voice coil positioned in the field of a permanent magnet. Lorentz force oscillates in the same phase and frequency as the current generated by the sound radiation, and it is commonly accepted that membrane vibrates with amplitude being linearly dependent on the amplitude of the input AC signal, while natural frequency is expected to be independent upon vibration amplitude, i.e. the system operates in a linear regime. However, this is true only for small driving AC currents (<10 mA), whereas for higher currents vibration amplitude deviates from the linear dependence and natural frequency changes with changing amplitude of the input signal. It is of great importance to study such a nonlinear system in terms of laws and rules of widely quoted nonlinear phenomena, including stability theories. Their great development in past decades makes possible the use of new physical tools in understanding the loudspeaker vibration properties. Thus an improved understanding of the dynamics of a loudspeaker is of great importance, since loudspeaker might be adequately redesigned and yield significantly better performance in an audio playback system.

Received 22 November 2006,
accepted 13 June 2008.

Chaotic state in dynamical systems is represented by a set of nonlinear equations [1] given in the form

$$\frac{\mathrm{d}\psi_i}{\mathrm{d}t} = F_i(\psi_1 \ldots \psi_2), \qquad i = 1, \ldots, N, \tag{1}$$

which might be applied to nonlinear forced oscillator [2] described by equation of motion

$$a\frac{\mathrm{d}^2x}{\mathrm{d}t^2} + b\frac{\mathrm{d}x}{\mathrm{d}t} + kx = f_1 = f_0\cos\varphi,$$
$$\varphi = \psi_2 = \omega t, \qquad \psi_1 = \frac{\mathrm{d}x}{\mathrm{d}t}. \tag{2}$$

In the linear regime when electrodynamic loudspeaker (EDL) is driven by small current ($I_0 \sim 10$ mA) coefficients in equation (2) are nearly constant, and stiffness $k$ is expressed by natural frequency $\omega_0$ and mass $M$ in the form $k = \omega_0^2 M$. Solution to equation (2) can be expressed as $x = A\cos\omega t$.

In this form, displacement x in equation (2) properly describes only the motion of the voice coil, while the points on the membrane, because of its flexibility, suffer combined displacement $x+z$, $z$ being the solution of the Bessel equation [3]

$$\frac{\mathrm{d}^2z}{\mathrm{d}t^2} + E\cdot\Delta z = \rho\frac{\mathrm{d}^2z}{\mathrm{d}t^2} - E\left(\frac{\mathrm{d}^2z}{\mathrm{d}t^2} + \frac{1}{r}\frac{\mathrm{d}z}{\mathrm{d}r}\right) = f_2. \tag{3}$$

$E$ and $\rho$ are respectively Young modulus and density of the membrane polymeric material. Equation (3) expresses

force density coming from inertial and elastic shear term. After integration over the membrane volume both terms can be added to the left side of equation (2).

However, Bessel modes derived from equation (3) do not contribute to the intrinsic friction of the membrane, but such a friction results from the viscoelastic losses and these losses are being manifested by fluctuating membrane surface visible as tilts [4]. Such tilts are stochastic surface fluctuations and are associated to vibration modes having frequencies one or two orders of magnitude higher than loudspeaker's natural frequency.

In these experiments stiffness was evaluated from the static measurements by the use of calibrated loads and corresponding evaluation of membrane displacements. It was found that stiffness has a form $k = m + nx + px^2$ ($m = 930\,\mathrm{N/m}$, $n = -114 \cdot 10^3\,\mathrm{N/nm^2}$, $p = 32 \cdot 10^3\,\mathrm{N/m^3}$), and it is notable that $k$ obeys a minimum value at $x \sim 1.8\,\mathrm{mm}$. A short analysis of equation (2) showed that it would be exceedingly difficult to explain amplitude bifurcations and chaotic state in EDL by this nonlinearity, even if coefficients $m$, $n$, $p$ are varied in a broad range of values being far apart from the commonly accepted values indicated by technical performance of the loudspeaker. Instead, the only effect evaluated by the use of simulations based upon this quadratic nonlinearity was well known amplitude cutoff [5], continuously observed during the course of this work (inset of Figure 2). On the other hand, another experiment showed that membrane's properties play an important role in the dynamic system. The same membrane was reinforced by phenolic resin [6] leaving elastic suspension intact. Static measurement of the stiffness after the reinforcement revealed that $k$ increased to about 1230 N/m at origin, and this is to be contrasted to a concept of the EDL membrane as being a point mass suspended on an elastic spring. Furthermore, an increase of the stiffness by such reinforcement appeals an attention for a substantial contribution of membrane elasticity to the vibration properties of EDL, and in addition to elastic properties of the membrane governed by the Young modulus only, viscoelasticity of the composite polymer material plays an important role. Viscoelastic losses in the membrane are expressed by intrinsic membrane friction $R_i$ entering the second term to equation (2), and these losses are brought about as a hysteresis in stress-strain diagram of the membrane material. Systems with such hysteresis obey memory properties which manifest in EDL as a time dependent stiffness [7], and in the literature dealing with stochastic processes are commonly referred as to be after effect.

Furthermore, one has to consider that vibration amplitude dependent resonance frequency (Figure 3) deviates from the dependence of the resonance frequency calculated from the formula $k = \omega_0^2 M$, $k$ being measured statically by the use of the calibrated loads. Indeed, while an initial decrease of the calculated resonance frequency from static measurements, correlates to a decrease of resonant frequency obtained from dynamic measurements, a strong increase of the latter at $A > 5\,\mathrm{mm}$ might not be explained by simple quadratic nonlinearity in equation (2).

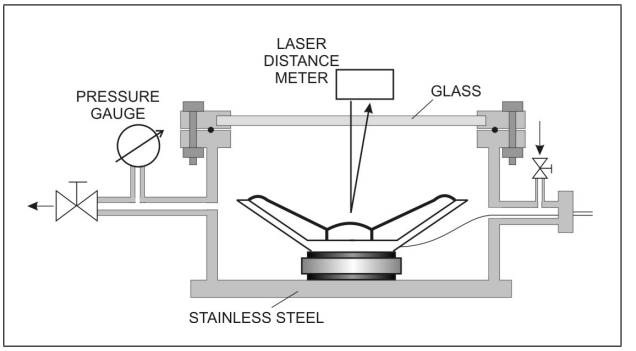


Figure 1. Experimental set-up with the loudspeaker, evacuation chamber and laser distance meter.

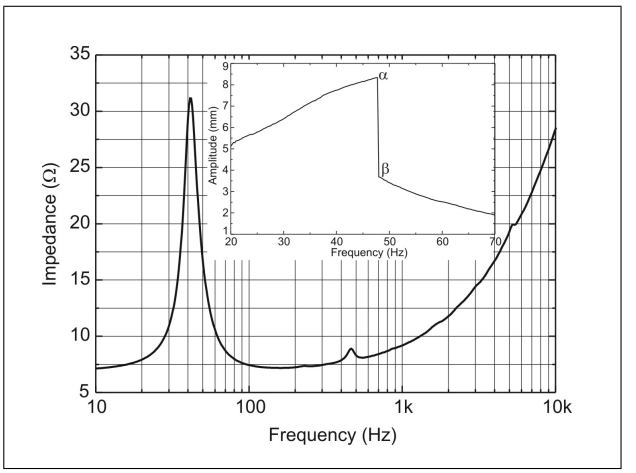


Figure 2. Frequency dependence of the impedance of the loudspeaker. Inset shows frequency dependence of the vibration amplitude for driving current $I_0 = 4\,\mathrm{A}$.

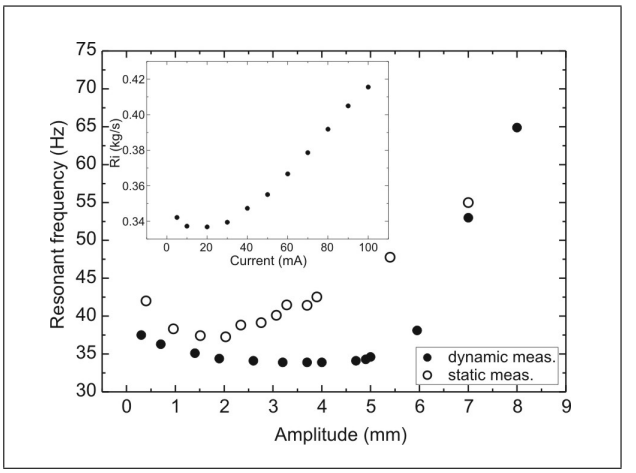


Figure 3. Amplitude dependent resonant frequency; (∘) calculated from the statically measured stiffness, (•) measured in dynamic regime. Inset shows current dependent intrinsic membrane friction $R_i$.

In this paper we present the bifurcation diagram of vibration amplitudes recorded experimentally in an EDL, and on an account of that we shall try to investigate the relevance of Bennewitz-Rötger (BR) theory [8], which strove

to explore forced vibration of the viscoelastic body. An important feature of BR approach is a natural extension of equation (2) with restoring term being renormalized by viscoelasticity. Finally, simulation calculations performed by the use of such an enhanced restoring term result in a bifurcation diagram of the vibration amplitudes with introductory parameters comparable to those given by the loudspeaker.

## 2. Experiment

Loudspeaker has been operated in a chamber of 5.2 liters in volume (Figure 1), having natural frequency of 965 Hz, and the chamber was evacuated by the use of the rotary vacuum pump. Glass window on the top of the chamber ensures the transparency to the beam emitted from the laser triangulation device which measures vibration amplitudes with 2 microns accuracy in the range 16–120 mm. The sampling time of the distance meter is around 0.9 milliseconds.

The experiments were performed in the loudspeaker with natural frequency $\omega_0/2\pi = 43$ Hz (measured at driving current 1 mA, in 1 bar air atmosphere), diameter was being $2R = 16$ cm, cone angle $2\theta = 120°$, voice coil resistance $R_{DC} = 8$ Ohm, $Bl = 3.9$ Tm, and RMS power 60 W. The mass of the membrane and voice coil, both detached from the loudspeaker frame, was $M = 14.1$ g. According to the manufacturer's data, voice coil inductance was $L = 0.9$ mH, and impedance contribution of the inductive part $\omega_0 L$ to the loudspeaker impedance can be neglected for driving frequencies <100 Hz. Frequency dependence of the loudspeaker impedance is shown in Figure 2, and commonly known resonance peak is accompanied by the second feature visible at 455 Hz, and in this work agreed as being a viscoelastic resonance. Laser distance meter is equipped with 8 bits AD converter, which allowed the acquisition of 128 amplitude levels in up and down vibration directions. Output signal was captured by SR 785 spectrum analyzer, and transferred to Matlab for reading of vibration amplitudes.

The amplitude and impedance measurements were performed in an evacuated chamber, in order to remove the friction coming from air viscosity and turbulence, and this in turn enables an accurate evaluation of the intrinsic membrane friction Ri. For lower driving currents ($I_0 <$ 100 mA) intrinsic friction was calculated from the real part of the impedance at resonance frequency $\omega_R$, and $R_i$ enters the expression $Z_{re} = B^2 l^2 / R_i$, where voice coil resistance is subtracted. Dependence of $R_i$ on driving current is shown in the inset of Figure 3.

In a highly nonlinear regime ($I_0 > 1$ A) the resonance curve of the vibration amplitude deforms with increasing driving current, which is indicated by more asymmetric dependence on frequency, and for $I_0 = 1.85$ A amplitude suddenly drops [5]. This downturn is more pronounced for higher driving currents, like one depicted in the inset of Figure 2 for $I_0 = 4$ A. After the cut-off, as driving frequency changes, loudspeaker undergoes unstable

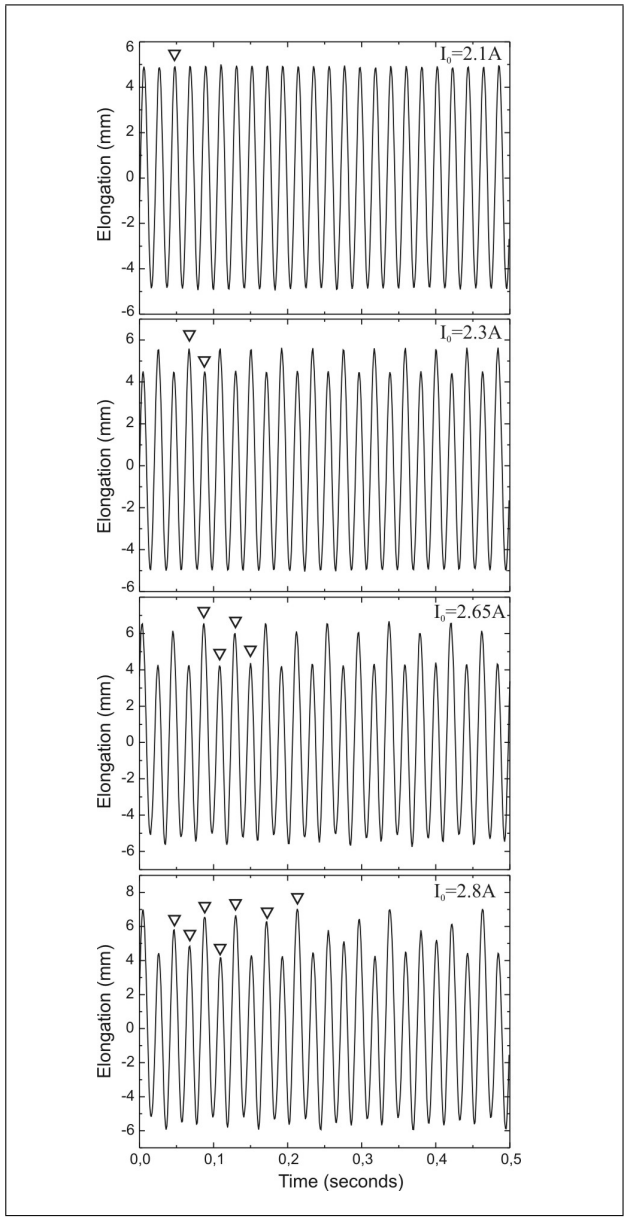


Figure 4. Time dependent elongation at frequency $\omega/2\pi = 48$ Hz, for different driving currents.

state characterized by an erratic behaviour of the amplitude, which is usual precursor of the chaotic state in the vibrating system. By an increase of the driving frequency unstable range was extended up to 10 Hz above the cut-off frequency, and within this range frequency was chosen, at which driving current sweep was applied for generation of bifurcations and subharmonic sequences.

The time dependent elongation at driving frequency $\omega/2\pi = 48$ Hz, recorded in an evacuated chamber is shown in Figure 4; (a) shows the time dependent elongation at starting driving current $I_0 = 2.1$ A, and recorded signal exhibits nearly harmonic form indicated by only one vibration amplitude. Figures 4b, 4c and 4d show additional vibration amplitudes generated at higher driving currents (marked with triangles) and their number increases with the increasing current.

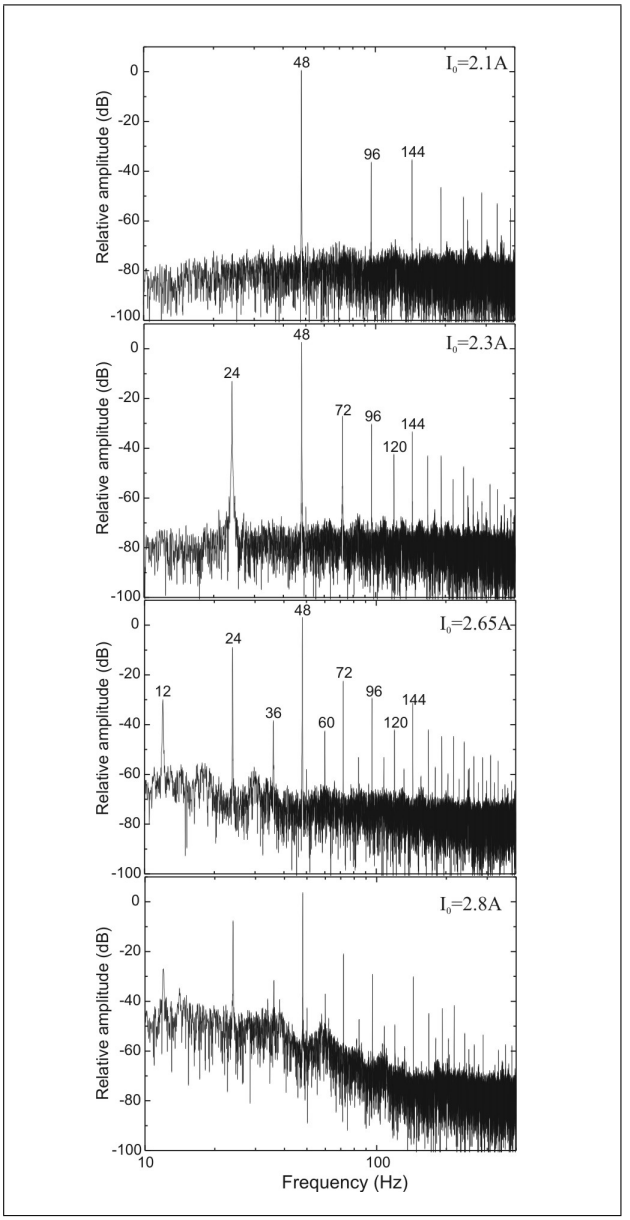


Figure 5. Average spectral analysis of recorded elongations shown in Figure 4.

Average spectral analysis of data indicated by Figure 4 is shown in Figure 5; (a) standard spectrum of nonlinear oscillator is visible [9], (b) increase of the driving current to $I_0 = 2.3$ A results in a period doubling and appearance of subharmonic at ½ 48 Hz, which is followed by the sequence indicated at higher frequencies by the multiples of 24 Hz, (c) next subharmonic is visible at 12 Hz, for driving current $I_0 = 2.65$ A, (d) process is extended to higher sequences, which in an averaging procedure of the spectrum analyzer, results to the spectral structure giving the appearance of being a white noise.

Measured vibration amplitude dependent on the driving current is plotted in the bifurcation diagram shown in Figure 6. The vibration amplitude for $I_0 = 2.1$ A is 5.2 mm and is nearly constant for this higher driving currents, while in the lower current range $0 < I_0 < 100$ mA vibration amplitude increases with the rate of 0.052 m/A. It is obvious that amplitude is heavily suppressed at high driving currents, and current dependent friction $R_i$ is insufficient to explain such a suppression, as one might be expected. In some instances, experimental findings appeared in the course of this work call an attention for the contribution of coupled friction-stiffness mechanism driven by membrane viscoelasticity.

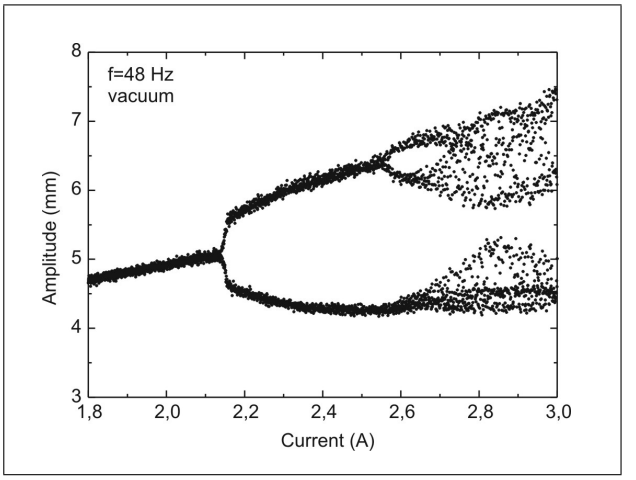


Figure 6. Amplitude versus driving current bifurcation diagram plotted from Figures 4 and 5.

## 3. Discussion

Viscoelastic losses in a vibrating body are associated with hysteresis in the stress-strain diagram, and loss of energy in the system is indicated by the area described within the hysteresis curve. The loss factor for the vibrating EDL system is expressed [10] as

$$\eta = \frac{W}{D}, \quad D = E_{el} + E_{kin}, \quad E_{in} = W + D. \qquad (4)$$

$W$ is energy dissipated during one period $T = 2\pi/\omega$, and $D$ is mechanical energy expressed as a sum of kinetic and elastic energy, the former being zero at maximum elongation $x = A$. It should be noted that the amplitude cut-off is associated with more rapid decrease of the elastic energy than of input energy, as a result of its quadratic dependence on the amplitude. Energy input $E_{in}$ for vibration amplitude before cut-off $A = 8.3$ mm (point $\alpha$ in the inset of Figure 2) in one half cycle amounts $BI_0lA = 130 \cdot 10^{-3}$ Joules, which should be compared to the elastic energy $E_{el}$ calculated from the statically measured stiffness $kA^2/2 \sim 81 \cdot 10^{-3}$ Joules, and corresponding loss factor is 0.6. Just after amplitude cut-off (point $\beta$), energy input is $\sim 58 \cdot 10^{-3}$ Joules, elastic energy $\sim 8.95 \cdot 10^{-3}$ Joules, and loss factor ~5.4. The comparatively small value of the elastic energy calculated after cut-off, and an increase of the loss factor suggest that predominant energy loss comes from the friction term in equation (2). However, an independent evaluation of the stress-strain diagram [5] performed on the membrane gave

for the hysteresis surface $\sim 3.4 \cdot 10^{-3}$ Joules, at maximum strain $y = 80$ microns, which corresponds to the vibration amplitude $A = 6.1$ mm, and this is far to low to explain the difference between input energy and stored elastic energy $kA^2/2$, both being calculated in the cut-off regime. On the other hand, energy dissipated by friction and expressed as $\omega R_i A^2$ should require $R_i \sim 9.3$ kg/s, which is not visible as a possible broadening of impedance or amplitude resonance curves. The evaluated and measured data suggest a systematic reconsideration of equation (2), not only in far anharmonic regime, but also in a low nonlinear regime in which an ordinary loudspeaker operates.

Bennewitz and Rötger proposed [8] a rather simple model of the viscoelastic body subjected to the forced oscillation, and the body was supposed to consist of a large number of small viscoelastic regions, each region being the source of the local hysteretic surface deformation. Deformation $y_i$ of the $i$-th region is relaxed to the equilibrium in time $1/\gamma_i$, and particular $\gamma_i$ might be interpreted as viscoelastic resonance frequency. Assuming the local deformation $y_i$ of the membrane, the general BR equation of motion is given by

$$\sum_j^n \alpha_j \left[ y^{(n)} + \sum \gamma_k \gamma_l y^{(n-2)} + \cdots + \gamma_k \gamma_l \ldots y^{(1)} \right] - \prod_j \gamma_j G = f_3. \qquad (5)$$

This model applied to the EDL pictures membrane deformation as decomposed into set of local surface fluctuations $y_i$ coming from the buckling, stretching and shear strains and these fluctuations are relaxed according to

$$y_i = \mathrm{e}^{-\gamma_i t}. \qquad (6)$$

In the first approximation the maximum tilt strain $y$ on the membrane surface is is assumed to be linearly dependent on the average vibration amplitude.

In fact, BR model is analogous to the Maxwell model of viscoelasticity [11] based upon a picture of $n$ springs and dampers connected in series, each spring-damper combination corresponding to one small surface region.

When mean statistical value of $\gamma_i = \gamma$ is assumed, BR equation reduces to a simpler form [12], and force per unit mass is expressed as

$$\frac{1}{\omega_0}\frac{\mathrm{d}^3 y}{\mathrm{d}t^3} + \frac{\gamma}{\omega_0}\frac{\mathrm{d}^2 y}{\mathrm{d}t^2} + \omega_0\left(1 + \frac{\beta\delta}{E}\right)\frac{\mathrm{d}y}{\mathrm{d}t} + \omega_0 \gamma y = F. \qquad (7)$$

$\omega_0$ is natural frequency of the vibrating system consisting of the membrane and its suspension. Assuming this contribution, the total force experienced by a particular point on the membrane surface is $f_1 + f_2 M/\rho + FM$.

Viscoelastic resonance frequency is given [13] by $\gamma = K\nu/d^2$; $\nu$ being kinematic viscosity of the membrane material and $d$ is membrane thickness. $K$ is dimensionless form factor, and $K \sim 1$ for a thin plate of very large diameter, while it is considerably reduced for conical geometry of the membrane. $E$ is Young modulus of the membrane material $\beta$ is elastic stiffness of the membrane, and $\delta$ is a constant depending on the membrane dimensions.

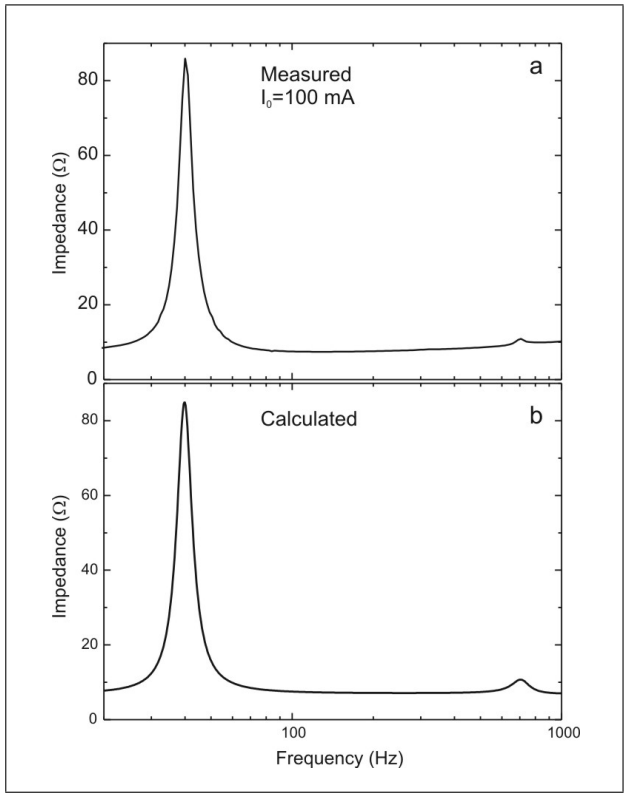


Figure 7. Electric impedance; (a) measured, and (b) calculated from 4th order Bennewitz-Rötger equation.

Equation (7) stresses an important coupling of the elastic stiffness to the internal friction $R_i$, and resonance frequency increases with increasing vibration amplitude faster than it should be expected from the statically measured stiffness as it is shown in Figure 3. Viscoelastic resonance indicated by the second feature in the impedance–frequency diagram (Figure 2), and in these experiments $\gamma = 455$ Hz at $I_0 = 100$ mA ($R_i = 0.42$ kg/s,). Linear extrapolation of $\gamma$ at $R_i \sim 1.1$ kg/s, a value estimated before cut-off, gives for elastic energy at cut-off amplitude $A = 3.7$ mm $E_{el} = \omega\gamma M A^2/2 \sim 38.1 \cdot 10^{-3}$ Joules at $I_0 = 4$ A, and this result matches much better the energy difference discussed above. The remaining discrepancy of as much as $12 \cdot 10^{-3}$ Joules may come from the neglected increase of hysteretic dissipation after cut-off and from the omission of the elastic shear contribution in Bessel equation (3).

The model of an enhancement of the restoring force by intrinsic friction was further supported when an extension of BR equation up to 4th order was being done, and solutions to corresponding ordinary differential equation [14] result in two resonance peaks, as it is shown in Figure 7. Relative distance of two peaks on abscissa is not an adjustable parameter in calculation and is in a fair agreement with experiment. Furthermore, solution to such an equation [14] indicates the anomalous current dependence of the resonance frequency presented in Figure 3, and such

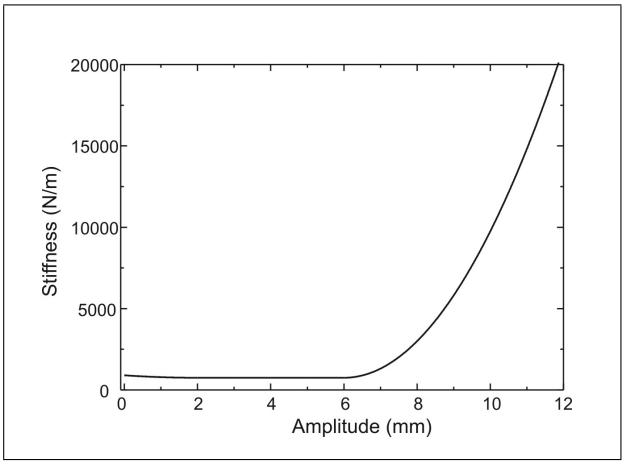


Figure 8. Model of the elastic stiffness dependent on the vibration amplitude used for the evaluation of bifurcation diagram indicated by Figure 9.

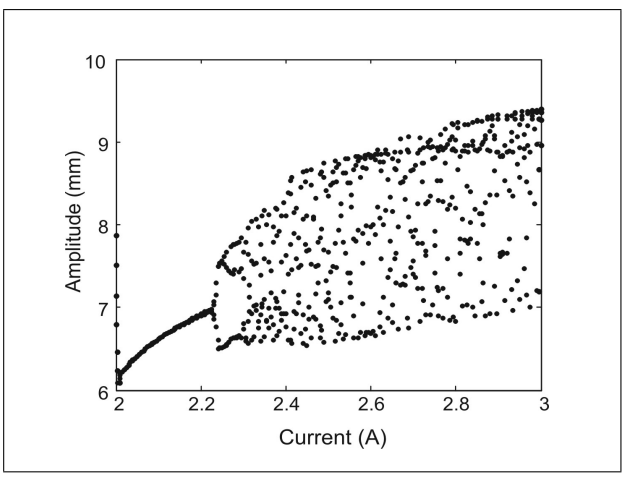


Figure 9. Simulated bifurcation diagram for elastic stiffness shown in Figure 8.

dependence suggests the modeling of elastic stiffness as being shown in Figure 8. The solution to equation (2) with such a supposed amplitude dependent stiffness evaluated by the use of the Runge-Kutta Matlab technique is shown in the Figure 9. Simulated diagram clearly indicates increasing number of bifurcations with increasing driving current. The initial conditions of displacement and velocity for the first excitation amplitude were assumed to be zero, while initial conditions for each next excitation current, were assumed as to be last integration points from the previous current step. It is noteworthy that the lowest slope of the stiffness necessary for occurrence of bifurcations is that just presented in Figure 8, and its rather high value is in agreement with the slope calculated from the formula $k = \omega_0 \gamma M$.

It is worthy to note that BR model is mechanical analogue of the more general principle, associated also with turbulence [15] and ferromagnetism, when energy invested to the large scale nonlinear system is transferred to many smaller regions which disperse it to heat by viscous action. Hysteretic dissipation in ferromagnetic material is accomplished in domain walls. Similarly, it might be expected that Bessel mode deformation of membrane, playing the role of a large scale system, is chopped in a number of small dissipative parts represented by surface tilting. By the use 3D laser scan methods such tilt structure has being made visible [4] on the membrane surface, suffering concentric deformation, in agreement with Bessel mode deformation. In the course of Bessel mode deformation, membrane dissipates no energy irreversibly, but deformation is directed toward the instability, which could terminate to its possible fracture. Instead, such instability is prevented by nonlinear dynamical system which transfers dissipation to small tilt subsystems, being analogous to BR regions.

## 4. Conclusion

An experimental evidence of the chaotic state in an electrodynamic loudspeaker has been presented, and in contrast to commonly accepted picture when such state appears by solution of Duffing equation with statically measured elastic stiffness, a model of viscoelastic coupling is proposed for explanation of observed phenomena. Viscoelastic coupling renormalizes elastic stiffness by factor $2\pi\gamma/\omega_0 \sim 10.6$, and $\gamma = 455\,\mathrm{Hz}$ is the viscoelastic resonance frequency. The measured and evaluated data suggest such a coupling even in the case of comparatively small driving currents when the loudspeaker operates in a weakly anharmonic regime present already in a usual sound reproduction. The coupling of intrinsic membrane friction to the elastic stiffness has been verified by analysis of Bennewitz-Rötger equation dealing with forced vibration of a viscoelastic body, and calculated data are in a satisfactory agreement with measurements.

### References

[1] E. Ott: Chaos in dynamical systems. Cambridge University Press. 2nd Edition, 2002.

[2] P. M. Morse: Vibration and sound. Acoustical Society of America, 5th printing, 1995.

[3] G. L. Baker, J. P. Gollub: Chaotic dynamics: an introduction, 2nd edition. Cambridge University Press, 1996. p.39.

[4] M. Colloms: High performance loudspeakers, 6th edition. John Wiley and Sons, 2005. p.478.

[5] L. D. Landau, E. M. Lifshitz: Fluid mechanics. 2nd edition, course of theoretical physics, volume 6. Elsevier, 2004. p.84.

[6] I. Djurek, A. Petošić, D. Djurek: Mass nonlinearity and intrinsic friction of the loudspeaker membrane. 122nd AES Convention, Vienna, Austria, May 5-8, 2006, Convention paper 7075.

[7] W. Klippel: Dynamical measurement of loudspeaker suspension parts. 117th AES Convention, San Francisco, USA, October 28-31, 2004, Convention paper 6179.

[8] K. Bennewitz, H. Rötger: Ueber die innere Reibung fester Körper; Absorptionsfrequenzen von Metallen im akustischen Gebiet. Physik. Zeitschr. **37** (1936) 578–588.

[9] T. von Kármán: The engineer grapples with nonlinear problems. Bulletin of the American Mathematical Society **46** (1940) 615–683.

[10] E. E. Ungar, J. E. M. Kerwin: Loss factors of viscoelastic systems in terms of energy concepts. J. Acoust. Soc. Am. **34** (1962) 954–957.

[11] A. S. Wineman, K. R. Rajagopal: Mechanical response of polymers, an introduction. Cambridge University Press, 2000. p.28.

[12] M. Päsler: Ueber einen Zusammenhang der Bennewitz und Roetgerschen Theorie der inneren Reibung mit der von Päsler. Zs. F. Phys. **124** (1946) 105–117.

[13] D. R. Bland: The theory of linear viscoelasticity. Pergamon Press, New York, 1960.

[14] A. Petošić, I. Djurek, D. Djurek: Modeling of an electrodynamic loudspeaker including membrane viscoelasticity. 124th AES Convention, Amsterdam, The Netherlands, May 17-20, 2008, Convention paper 7356.

[15] G. Stolovitzky, K. R. Sreenivasan: Kolmogorov's refined similarity hypotheses for turbulence and general stochastic processes. Rev. Mod. Phys. **66** (1994) 229–240.